A Conjecture Concerning the Symmetries of Planar Nets and the Hard disk Freezing Transition†

John J. Kozak,‡,|| Jack Brzezinski,§ and Stuart A. Rice*

Department of Chemistry, DePaul University, 243 South Wabash Avenue, Chicago, Illinois 60604, AHA Communications Inc., 151 North Michigan Avenue, Chicago, Illinois 60601, and Department of Chemistry and The James Franck Institute, The University of Chicago, 929 East 57th Street, Chicago, Illinois 60637

Received: July 16, 2008; Revised Manuscript Received: September 19, 2008

We examine the conjecture that in a 2D system of hard disks the packing fraction at which the continuous transition from the ordered 2D solid to the hexatic phase occurs, and that at which the very weak first-order or continuous transition from the hexatic to the fluid phase occurs, can be correlated with the packing fractions of patterned networks (tessellations) of disk positions that span the 2D space. We identify three tessellations that have less than close packed density, span 2D space, and have percolated continuity of disk−disk contact. One has a packing fraction of $\eta = 0.729$, very slightly larger than the estimated packing fraction at the ordered solid-to-hexatic transition, $\eta = 0.723$, and the other two have packing fractions of $\sim$0.680, slightly smaller than that identified as the upper end of the stability range of the liquid phase, $\eta = 0.699$. The region $0.680 < \eta < 0.729$ is identified with the hexatic domain. The end points of this region can be placed in correspondence with nets for which the defining unit structures are regular polygons, but not the hexatic domain, in which there are randomly dispersed clusters that need not be regular polygons. The densities at which the percolated tessellations span the 2D space are regarded as special points along the density axis. We suggest that the possibility of forming different symmetry nets with sensibly the same packing fraction is a geometric analogue of a bifurcation condition that divides the configuration space into qualitatively different domains, and that the onset and end of the hexatic region are correlated with such divisions of the configuration space.

I. Introduction

Although first observed in computer simulation almost fifty years ago[1,2] and intensively studied since then, there remain unsettled aspects in our understanding of the melting/freezing transition in a two-dimensional (2D) system of hard disks. It is known that thermal fluctuations destroy the long-range positional order of a 2D system. However, the system can still be highly ordered locally and form a 2D solid with quasi-long-range positional order and long-range orientation order. One of the consequences of the loss of the long-range positional order in the 2D solid is that the character of the freezing transition appears to be fundamentally different from that in three dimensions (3D). Indeed, the most widely accepted theory of 2D melting predicts that a 2D system that supports only one ordered solid phase melts via sequential continuous phase transitions, whereas a 3D system always melts via first-order transition with a discontinuous change in density.

The study of 2D phase transitions has been greatly enriched, overall, by examination of the hard square[3] and hard hexagon[4] lattice gases. In the former, an occupied site in a square lattice prohibits occupation of the four nearest neighbor sites and in the latter an occupied site in a triangular lattice prohibits occupation of the six nearest neighbor sites. In both cases there is a continuous transition from the disordered state to an ordered state at a critical density. Squares and hexagons match the fundamental symmetries of the square and triangular lattices, respectively; they can be packed so as to completely fill the 2D space. Pentagons and heptagons cannot be packed so as to completely fill the 2D space because they do not have symmetries that match any regular lattice. Simulation studies by Frenkel and co-workers[5] lead to the conclusion that in these cases the disordered fluid undergoes a (likely) continuous transition to a phase with the particle centers on a triangular lattice and random orientation of the pentagons (heptagons), and then a first-order transition to an ordered solid with antiparallel rows of ordered pentagons (heptagons).

We now return to the 2D hard circle (disk) system. Just as is the case for hard pentagons and heptagons, hard disks cannot be packed so as to completely fill the 2D space. The simulation data reported by Alder and Wainwright[1] showed that the 2D hard disk freezing transition occurs at a density that is considerably smaller than the density of closest packing, and their data suggested that the hard disk liquid-to-solid transition is first order. However, the determination of the character of the 2D freezing transition is very sensitive to the size of the simulation sample. The results of the most recent large-scale simulations of a dense 2D hard disk system (4×10^6 disks), reported by Mak,[6] imply that the melting process consists of a continuous transition from the ordered 2D solid to the hexatic phase (see below) at a packing fraction close to 0.723, and either a very weak first-order or a continuous transition from the hexatic to the fluid phase at a packing fraction close to 0.699.

The Kosterlitz, Thouless, Halperin, Nelson and Young (KTHNY) theory[7−11] of 2D melting is based on a characterization of the 2D solid as a deformable medium with inclusion of the two classes of point topological defects with smallest excitation energy to mediate structural changes; it relates the

† Part of the "Karl Freed Festschrift".
‡ DePaul University.
|| The University of Chicago.
§ AHA Communications Inc.

10.1021/jp806287e CCC: $40.75
Published on Web 11/01/2008

melting process to the mechanical instability of the 2D solid. Although the theory allows for other possibilities, it is commonly taken to predict that a 2D system that supports only one-ordered solid phase melts via sequential continuous phase transitions. The first transition is from the solid with quasi-long-range positional order and long-range bond orientation order to a hexatic phase with short-range positional order and quasi-long-range bond orientation order. This transition is driven by the dissociation of bound dislocation pairs in the solid. The second transition transforms the hexatic phase to the liquid phase in which both positional and bond orientation order have short-range; it is driven by the dissociation of individual dislocations to form disclinations.

What can we learn from comparison of the character of the phase transitions in 2D systems of hard polygons and hard circular disks? The results cited hint that there can be a correlation between the character of transitions in a 2D hard particle system and the packing symmetries and coverage of the 2D space that particular hard particles can sustain. In this paper we ask if this hint provides any insight. Specifically, we examine the conjecture that in a 2D system of hard disks the density at which the continuous transition from the ordered 2D solid to the hexatic phase occurs, and that at which the very weak first-order or continuous transition from the hexatic to the fluid phase occurs, can be correlated with the packing densities of patterned networks (tessellations) of disk positions that span the 2D space. We do not assert that such a correlation implies the actual occurrence of those tessellations, nor that there must be exact coincidence of the solid-to-hexatic and the hexatic-to-liquid transition densities with the densities of those particular tessellations. We do suggest that each of the densities at which the solid-to-hexatic and hexatic-to-liquid transitions occur is a signature of the existence of a nearby tessellation that completely spans the 2D space.

The tessellations of disk configurations that we seek have less than close packed density yet maintain continuity of disk-disk contact (percolated contacts); they will exist only at particular values of the disk density, and their symmetries and packing fractions will be different at different disk densities. We regard the densities at which particular tessellations span the 2D space to be special points along the density axis, because the symmetries and packing fractions of the tessellations at higher and lower density are different.

A similar possible role for tessellation of the 2D hard disk system appears when one examines the structural consequences of increasing the density from a value in the dilute fluid regime to a value in the solid regime. As the density increases, the pair correlation function of the system develops structure associated with the geometry of the excluded volume. At first only a broad nearest neighbor peak appears in the pair correlation function but ultimately, at high density, that function consists of narrow nonoverlapping peaks representing successive shells of disks in the ordered solid phase.[12] Near the freezing transition, but still in the fluid phase, the second maximum of the pair correlation function displays a shoulder, which has been interpreted as a signature of a precursor ordered arrangement of a subset of disks associated with mutual caging of each disk by the three alternating nearest neighbors defined by the Voronoi tessellation of the disk configuration.[13−16] This interpretation leads us to ask if a change in character of the tessellation of the planar net that spans the 2D space provides a signature for the freezing transition?

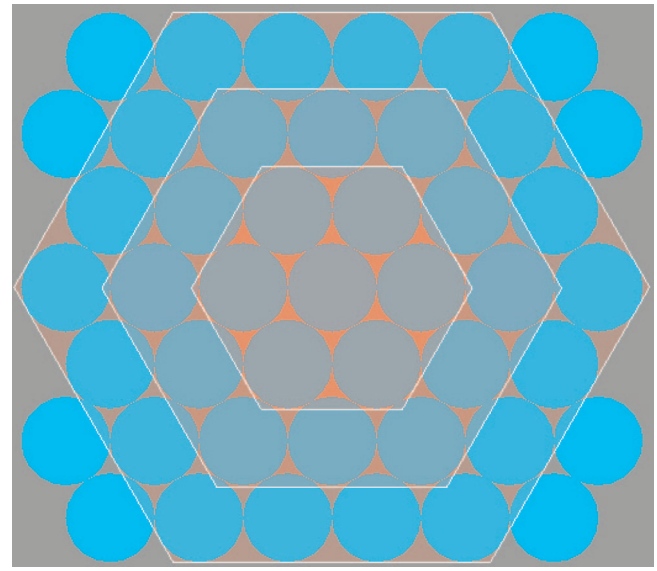

Figure 1. Extended array of n closest-packed hard disks, showing the first three ($k = 1-3$) nested hexagons, $n = 3k^2 + 3k + 1$.

Finally, to close the loop in our arguments we ask if 2D tessellations with different symmetries can be transformed continuously one into the other?

II. Two-Dimensional Tessellations

We wish to construct a set of tessellations of 2D disk configurations that have the following properties:

(i) the density of disks is less than that at closest packing;

(ii) each disk is in contact with two or more other disks and the tessellation spans the system.

To carry out this construction, we take advantage of the proof by Gauss, later refined by Fejes Toth, that the densest possible packing of circles in the plane generates a triangular (hexagonal) lattice.[17] When completely filled, this lattice has a packing fraction:

$$\eta(cp) = \frac{\pi}{\sqrt{12}} = 0.90690 \qquad (1)$$

To identify tessellations with the properties stated above, we examine the construction of lattices by replication of hexagonal arrays with different numbers of disks. This constructive procedure is not unique, and it cannot be claimed to identify all possible tessellations that meet the stated criteria, but it does draw on our knowledge of the structure of the closest packed tessellation. Our starting point is an array of seven disks enclosed by a hexagon from which we remove, sequentially, one, two,..., disks and then enclose the remaining disks in the smallest possible regular hexagon. We examine the symmetries and packing fractions of tessellations generated by repetition of these smallest hexagons. We will then designate a tessellation by the network symbol that specifies the sequence of faces that exists at each vertex (location of a disk center). With this notation, for example, [4.8.8] specifies that there are one square and two octagons that meet in cyclic order at a vertex in the net. The polygons that meet at the vertex need not be regular.

Consider the seven disk configuration diagrammed in the center of Figure 1; in the closest packed configuration the hexagonal perimeter that forms the convex hull of the assembly of particles is a regular polygon with all angles equal and all

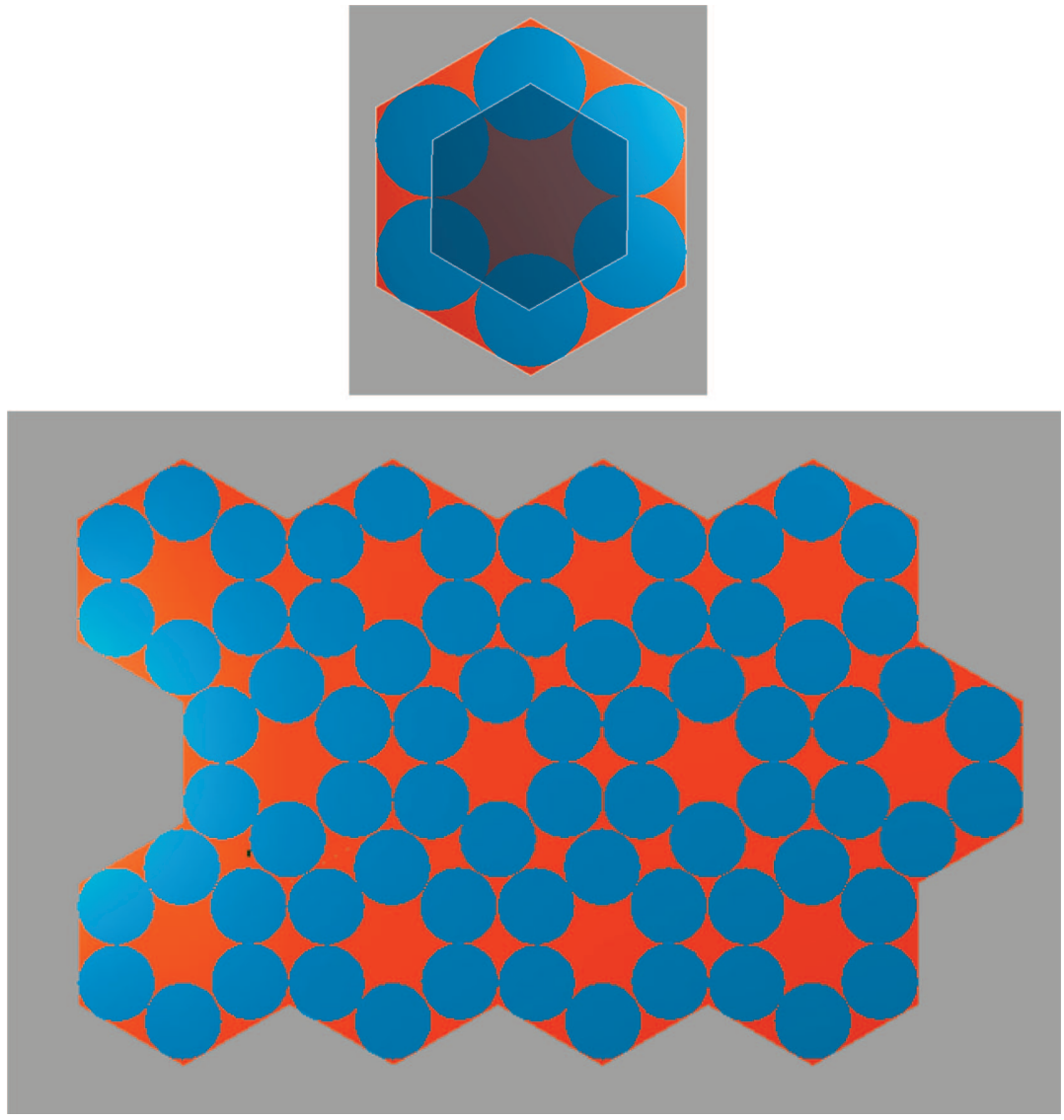

Figure 2. Case $n = 6$ hard disks in the smallest confining hexagon.

sides of the same length, s. Replication of this hexagonal unit generates an extended space-filling array. It can be shown[18,19] that if n nonoverlapping unit disks in R^2 are arranged so as to minimize the area of their convex hull, that convex hull tends to be "as hexagonal as possible". Indeed, regular hexagonal hulls occur for numbers of disks that satisfy[20]

$$n = 3k^2 + 3k + 1 \qquad (k \text{ an integer}) \tag{2}$$

The values $k = 0, 1, 2, 3,...$ then define a sequence of nested hexagonal units, displayed in Figure 1 for $n = 1, 7, 19, 37$. With respect to configurations of n unit disks packed inside the smallest encompassing regular hexagon of side s, straightforward calculation shows that

$$s = 2k + \frac{2}{\sqrt{3}} \qquad (k \text{ an integer}) \tag{3}$$

Although replication of the smallest hexagonal hull generates a space-filling pattern, the packing fraction of disks inside the smallest hull is not the same as the packing fraction in the infinite lattice because the boundaries of the smallest hexagonal hull do not define the unit cell of the lattice. The consequence of the choice of hexagonal hull rather than unit cell to generate the lattice is the incorporation in any finite lattice of small "pockets"; the correct packing fraction for the infinite lattice is approached as the size of the hexagonal hull is increased to include more and more disks. Thus, using eq 3, the packing fraction corresponding to the sequence of hexagonal units characterized by $k = 1-3,...$ approaches that for the infinite 2D system (asymptotically) with increase in k [for example, for $k = 1$, $\eta(n=7) = 0.85051$, for $k = 2$, $\eta(19) = 0.86466$; for $k = 3$, $\eta(37) = 0.87401$; for $k = 10$, $\eta(331) = 0.89436$; and for $k = 100$, $\eta(30301) = 0.90551$].

We now take advantage of a result first noticed for the close packing of unit disks in equilateral triangles.[21] One can show that removing the central disk from any arrangement corresponding to eq 2 does not change the value of s. We show at the top of Figure 2 an arrangement of disks with the center disk removed. The packing fraction of this $n = 6$ configuration is

$$\eta(6) = 0.72901 \tag{4}$$

Replicating the unit hexagon corresponding to this arrangement, one generates the net [3.4.6.4] shown at the bottom of

Figure 2. The packing fractions of the unit hexagon and the infinite lattice, η(net6), are the same. We note that η(net6) is very slightly larger than the estimated packing fraction at the ordered solid-to-hexatic transition, $\eta = 0.723$. This small difference is consistent with the view, expressed by Mak,[9] that the transition density identified from the simulation data lies slightly inside the domain of stability of the hexatic phase.

The disk removal procedure introduced above can be continued: we sequentially remove disks from the $n = 7$ hexagonal unit and then determine the side length characterizing the smallest regular hexagon bounding the remaining disks. Replication of the consequent renormalized hexagon generates a planar network characterized by a specific packing fraction.

Although out of order, we now consider the case $n = 3$, after removal of four disks from the hexagon with $n = 7$. We jump to this case because, as for $n = 6$, the packing fraction for the bounding hexagon can be computed exactly. For the case $n = 3$, the value of s is

$$s = \frac{4}{\sqrt{3}} \tag{5}$$

and one finds

$$\eta(3) = 0.68017 \tag{6}$$

The tessellation generated in this case is shown in Figure 3; it is referenced in the crystallographic literature as the Kagome net; see O'Keeffe and Hyde.[22] We note that $\eta(3) = \eta$(net3) is slightly smaller than the packing fraction, $\eta = 0.699$, that Mak identifies as the upper end of the stability range of the liquid phase, and also slightly smaller than the packing fraction, $\eta = 0.686$, that Truskett et al.[12] and Huerta et al.[16] regard to be just below the freezing density.

Consider next the case $n = 5$. An exact analytic result for s is not available, but Friedman[23] has performed a computer-graphic minimization that yielded the value $s = 2.999+$. The packing fraction corresponding to this value of s is

$$\eta(5) = 0.6722 \tag{7}$$

Replication of the unit cell for this case, Figure 4, does not lead to an extended structure composed of regular polygons. However, examination of the net reveals that there are local configurations [5.4^3] and [5.4.3.4]. O'Keeffe and Hyde[22] describe an extended lattice having such configurations, namely [5.4^3, 5.4.3.4, 5.4^3, and $(5.4.3.4.)^2$]. A finite section of this

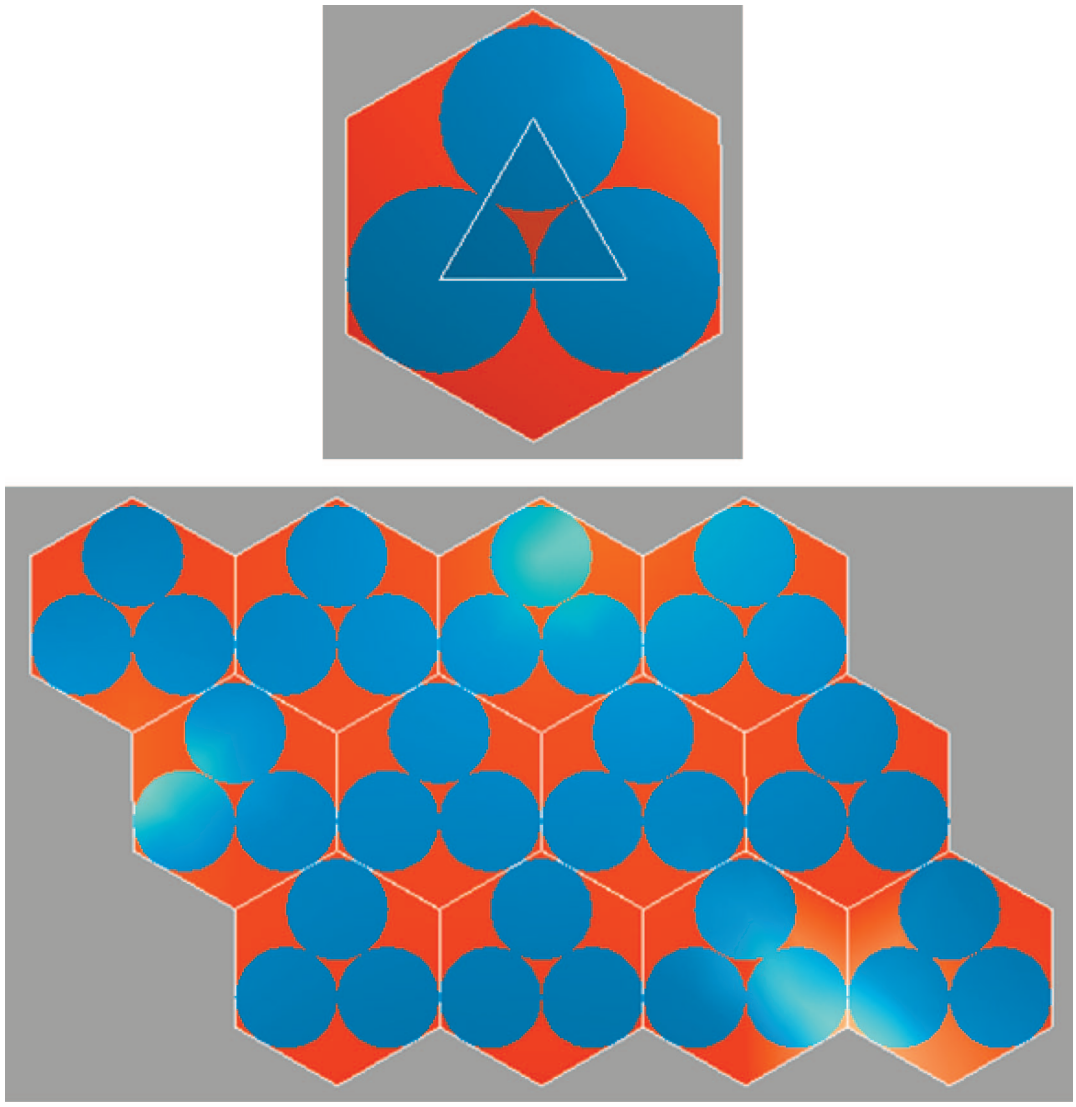

Figure 3. Case $n = 3$ hard disks in the smallest confining hexagon.

tessellation is shown in Figure 5. The polygons constituting this tessellation are not regular, but O'Keeffe and Hyde show that there is a set of "best covering" regular polygons that closely approximate those in the lattice. The packing fraction of the infinite lattice with those best covering, regular polygons is

$$\eta(\text{net5}) = 0.67747 \tag{8}$$

Turning now to the case $n = 4$, Manzoor[23] has determined a "best bound" for s to be

$$s = \frac{2}{\sqrt{3}} + \frac{4}{\sqrt{7}} \tag{9}$$

for which

$$\eta(4) = 0.68023 \tag{10}$$

Replication of the hexagonal unit generates the pattern displayed in Figure 6. It is notable that the values of the packing fractions for the cases $n = 4$ and $n = 3$ are essentially the same. If all but two hard disks are removed from the $n = 7$ hexagonal unit, the value of s can be determined exactly; it is

$$s = 1 + \frac{2}{\sqrt{3}} \tag{11}$$

Replicating the two-particle configuration generates an array resembling the lattice $[4.8^2]$, for which

$$\eta(\text{net2}) = \frac{\pi}{3 + 2\sqrt{2}} = 0.53912 \tag{12}$$

Because we are interested in a possible correlation between the densities at which changes in the symmetry of tessellation occur and the densities at which the ordered solid-to-hexatic and hexatic-to-fluid disk transitions occur, we will not pay any further attention to the lattice generated by $n = 2$. This lattice has an open structure and a packing fraction considerably smaller than that at the liquid-to-hexatic transition, and it will have entropy considerably smaller than that of the disordered fluid with the same packing fraction.

To connect the set of tessellations defined above with the successive phase transitions in the hard disk system, we note that, as the disk density is increased, the first appearance of possible extended percolated contact disk configurations with regular polygonal structure occurs for $n = 3$ and/or $n = 4$; both tessellations [referred to later in the text as nets 3 and 4, respectively] have a packing fraction of ~0.680. At the very slightly smaller packing fraction 0.677, there is the disk configuration with the irregular polygon structure identified for the case $n = 5$ [net 5].

We infer that the possibility of forming different symmetry nets with sensibly the same packing fraction is a geometric analogue of a bifurcation condition. At this density the system chooses between changing from a disordered state to a partially

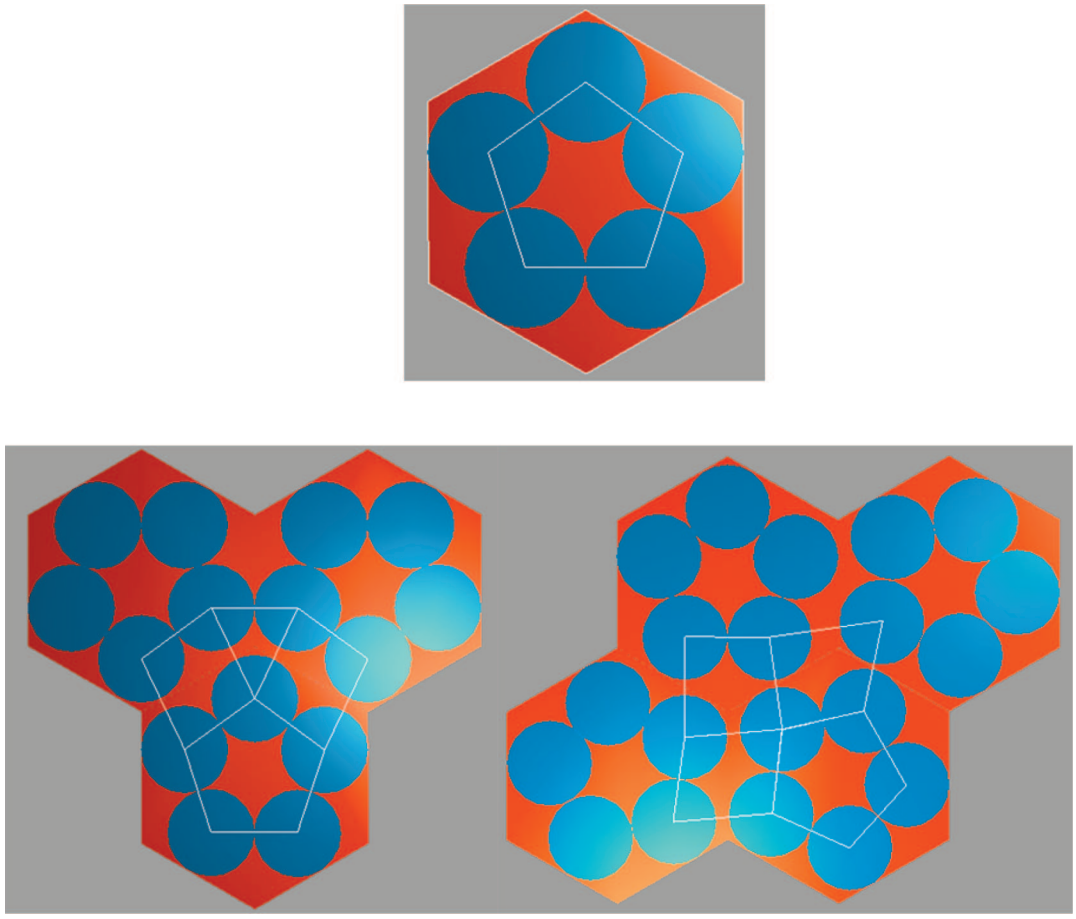

Figure 4. Case $n = 5$ hard disks in the smallest confining hexagon.

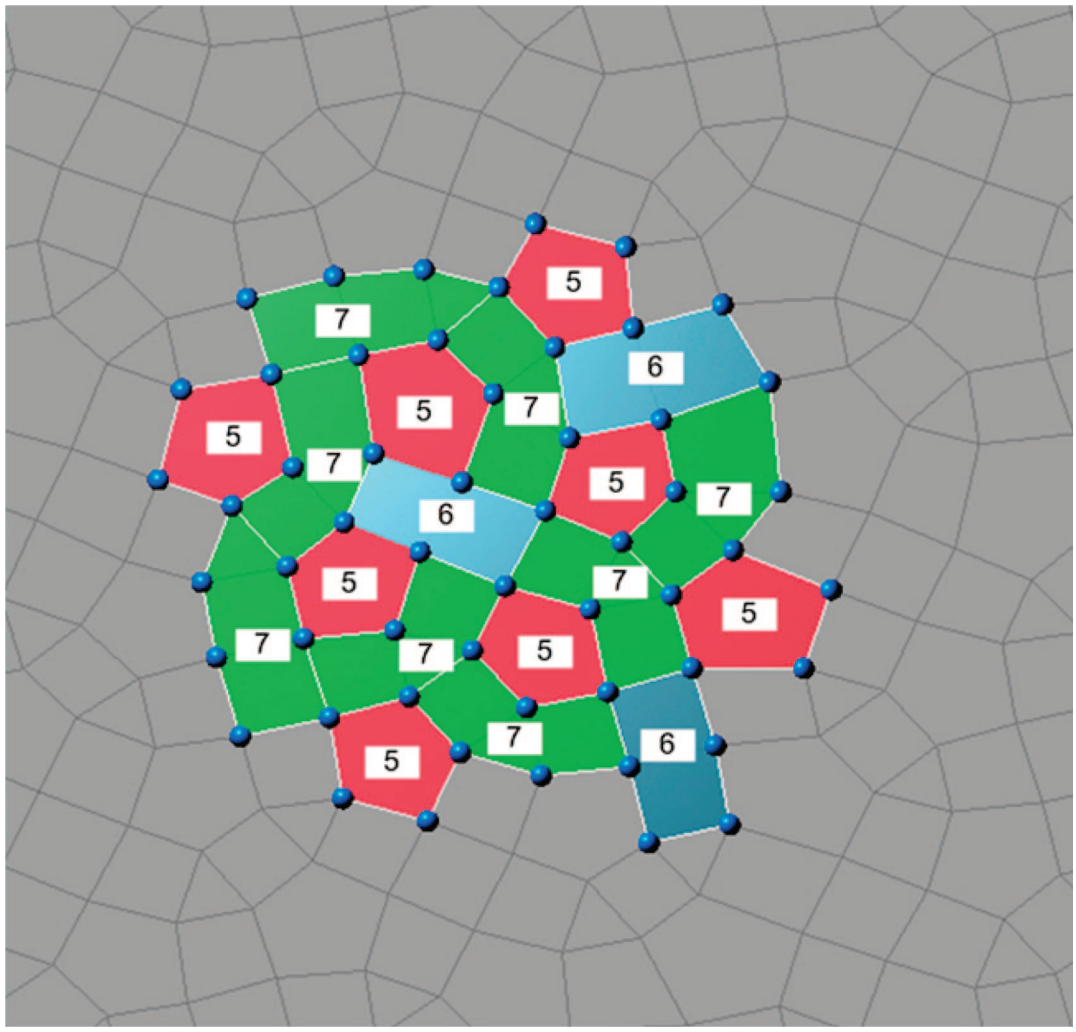

Figure 5. Extended array corresponding to $n = 5$ (net 5), showing regions of 7, 6 and 5 clusters.

ordered state or one of two ordered states. That is, viewing the space of possible disk configurations as a function of density, we argue that there is a critical density below which only disordered configurations are stable. It is not necessary that the system become ordered when the packing fraction is precisely that for net 3 and/or net 4 because other configurations with greater entropy exist at that density. Nevertheless, the value of the density for net 3 and/or net 4 divides the configuration space into qualitatively different domains, and we suggest that the onset of the hexatic region is correlated with that division of the configuration space.

We noted earlier that the hard disk melting transition occurs at a packing fraction considerably smaller than that of closest packing, 0.723 compared to 0.907. Because net 6 has the highest density of a tessellation that is less occupied than the closest packed triangular lattices, $\eta(6) = 0.729$, we suggest that disk rearrangement in a fully occupied triangular lattice is impossible until the packing fraction falls below that of net 6. We then suggest that the value of the density for net 6 also divides the configuration space into qualitatively different domains.

We now identify the region bracketed by the packing fractions 0.680 and 0.729 as the hexatic domain. Although the packing fraction end points of this region can be placed in correspondence with known crystallographic lattice nets for which the defining unit structures are regular polygons, this is not the case for the hexatic domain, in which there are randomly dispersed clusters where the constituent triples, quartets, pentagons, hexagons, etc., need not be regular polygons.

The above comments were based on an analysis of lattice arrays that were either periodic or quasi-periodic. However, it is possible that a decrease in packing fraction below a threshold value may result in a randomized array of disks that is not the patchwork quilt illustrated (locally) in Figure 5, but rather an array describing an aperiodic lattice. The best-known aperiodic lattice is the Penrose tiling,[24] for which Henley[25] has calculated the packing fraction to be

$$\eta(\text{Penrose}) = 0.738 \tag{13}$$

Although $\eta(6) = 0.729 < \eta(\text{Penrose}) = 0.738$, the hexatic domain configurations may also be correlated with aperiodic structure(s). It is worth noting that the ordering of the packing fractions of the lattices generated by the successive disk removal process is

$$\eta(\text{net6}) > \eta(\text{net4}) \approx \eta(\text{net3}) > \eta(\text{net5}) > \eta(\text{net2}) \tag{14}$$

which displays a surprising nonmonotonic dependence on n [Table 1]. We shall return to this point in section IV.

Finally, given our assertions that $\eta(\text{net5})$ and $\eta(6)$ divide the space of disk configurations into qualitatively different regions, we now ask if it is possible to construct a geometrical transformation that proceeds from the regular polygonal disk configurations that define the net [3.6.3.6] to the regular polygonal disk configurations that define the net [3.4.6.4] via a

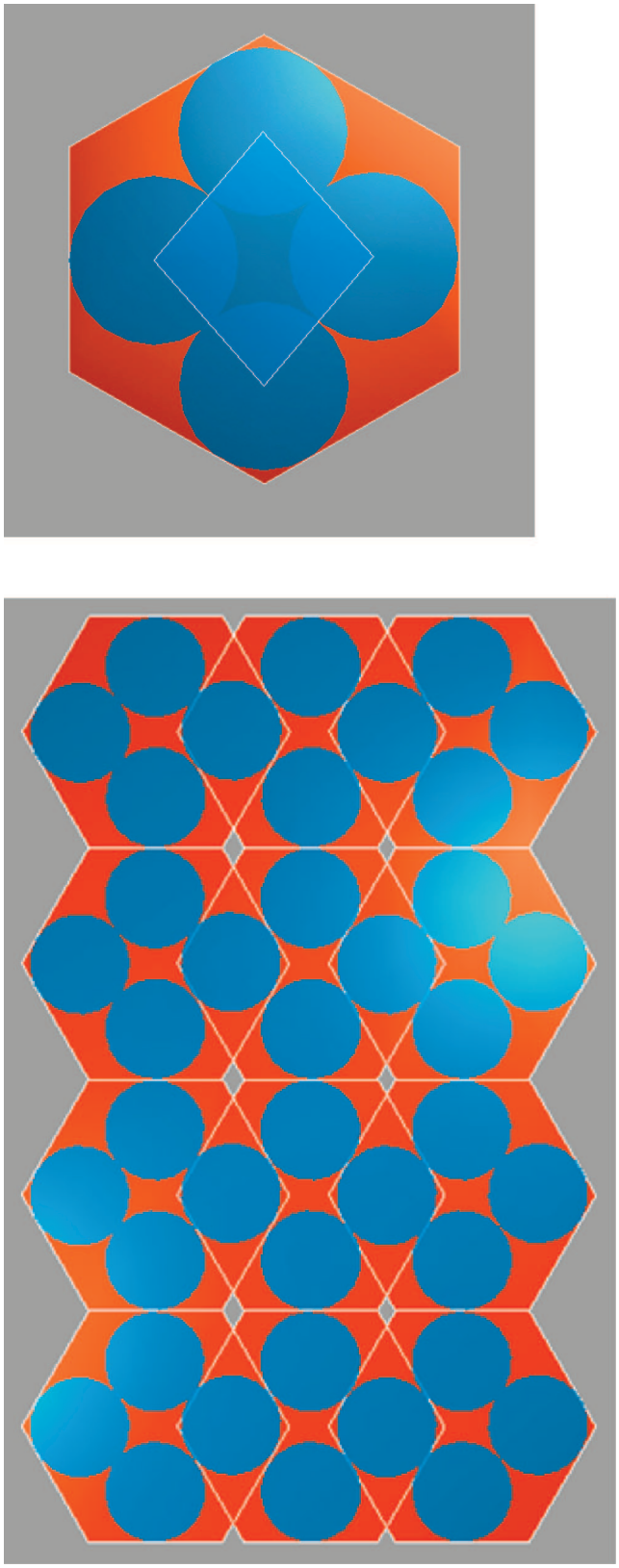

Figure 6. Case $n = 4$ hard disks in the smallest confining hexagon.

pathway that transits the planar net [5.4^3, 5.4.3.4, $5.4^3(5.4.3.4)^2$]; note that in the latter net the polygonal units are of (slightly) variable bond length and have variable internal angles. O'Keeffe and co-workers[22,26] describe how a given planar lattice structure can be transformed continuously, via the operations of contraction, dilation, rotation, vertex elimination and gliding, into other planar lattices. To visualize the transformation specified above,

TABLE 1: Packing Fraction for *n* disks in the Smallest Hexagonal Unit

n	packing fraction
7	0.850 511
6	0.729 009
5	0.672 226
4	0.680 230
3	0.680 175
2	0.520 900

we have (instead) designed a simulation (actually, a computer-generated mapping), which initializes incremental, random displacements of disks in the [3.6.3.6] net to transform that net to [3.4.6.4], mediated by a "disordered" configuration related to the planar net shown in Figure 3. [Details of the mapping are given in the Appendix.] We note that the mapping is reversible; i.e., it is possible to transit from the dense fluid to the crystalline phase, and crystalline phase to the dense fluid, with both deformations mediated by the same "disordered" configuration. Some of the stages in this transformation are displayed in the panels of Figure 7.

III. Free Volume in Two-Dimensional Tessellations

In a system of hard particles, a phase transition must be driven by a change in entropy, hence by a change in free volume. We now examine the free volumes associated with the various 2D tessellations described in the last section.

In 1960 Groemer[18] introduced a systematic way of characterizing the optimal packing of an arbitrary constellation of disks. A Groemer packing relates the area (A) enclosing the convex hull of a circle packing to the number n of disks inside it, and the perimeter (P). In 1968, Wegner[19] proved that the convex hull of a set of n unit disks is minimal when they are arranged in a Groemer packing. For all other possible packings, the theorem states that the associated area is

$$A > 2\sqrt{3}(n - 1) + (2 - \sqrt{3})\frac{P}{2} + \pi(\sqrt{3} - 1) \qquad (15)$$

One consequence of the Wegner theorem is that if n is a "hexagonal number" of the form given in eq 2, the Groemer packing forms a perfect regular hexagon. For example, the perimeter of the convex hull corresponding to a central disk surround by six other disks [the case $k = 1$ in eq 2] is $P = 18.283\ 185$, from which the area of the convex hull may be calculated using eq 15:

$$A(\text{convex hull}) = 25.533898$$

The area of the smallest bounding hexagon for seven disks, aligned as above, is

$$A(\text{minimal hexago n}) = 25.856407$$

Because the corners of the convex hull are "rounded," A(convex hull) is slightly less than A(minimal hexagon); the differences is 1.25%. Similarly, if one considers the case $k = 2$ in eq 2, i.e., the next largest convex hull, one finds $P = 6{\cdot}4 + 2\pi$, so that

$$A(\text{convex hull}) = 68.710812$$

which may compared with

$$A(\text{minimalhexagon}) = 69.033321$$

a difference of 0.47%. In terms of the problem at hand, we conceptualize the disk configuration in the two phase transition

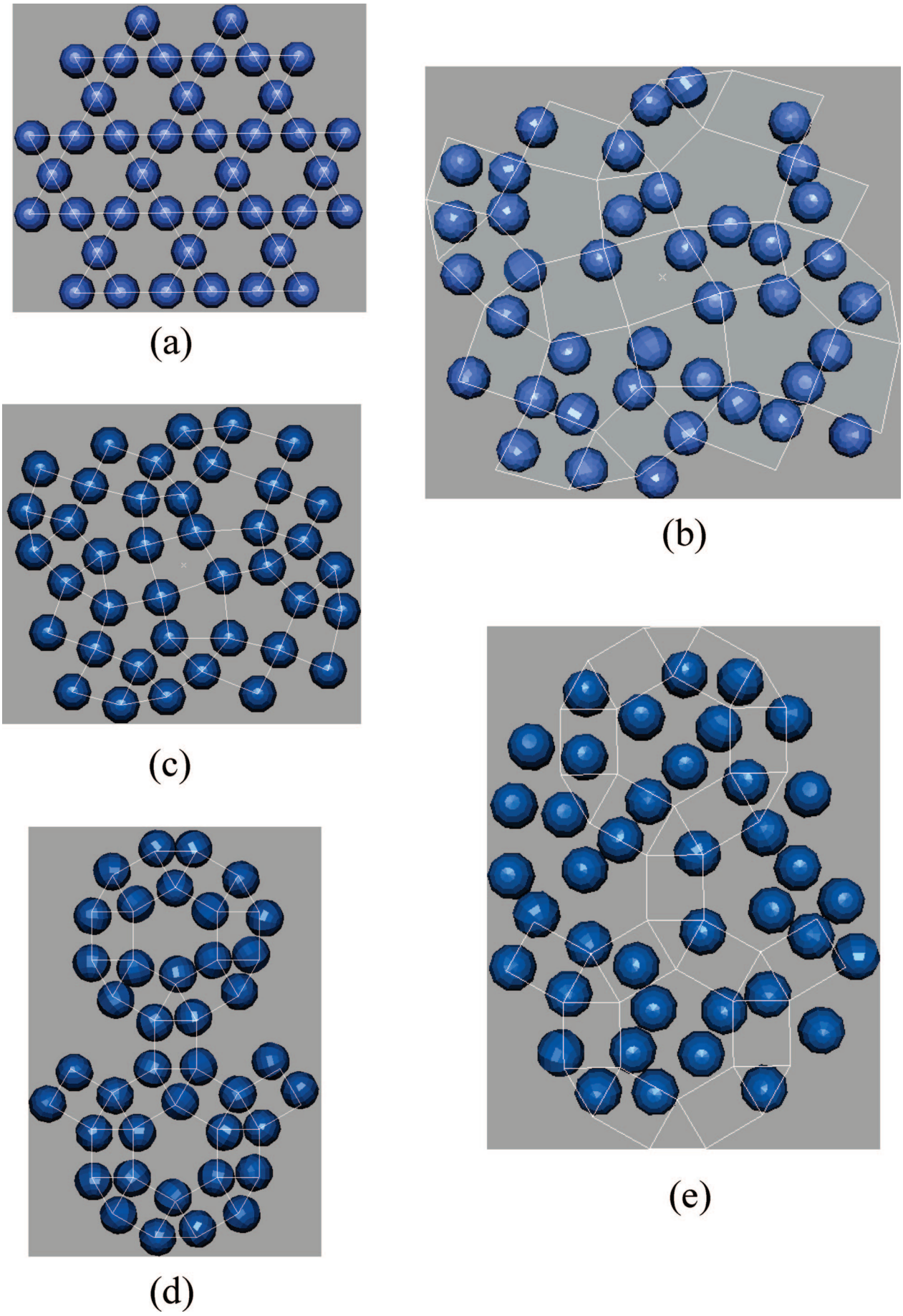

Figure 7. Sampling of representative stages in the transformation from tesselation [3.6.3.6] to tessellation [3.4.6.4].

region as consisting of domains containing arbitrary "patches" of disks, with the patches themselves likely irregular clusters. That is, we expect there to be irregular groups of disks, not all "close packed," or groups in which there are gaps along the perimeter, or holes inside the array. For each group of disks in the two-phase region, the convex hull can be delineated. The Wegner theorem guarantees that the area associated with such an arbitrary group will always be greater than that given by a Groemer packing of the same number of disks.

We now examine the values of A(convex hull) for each of the tessellations identified in the last section. The array we associated with the configuration geometry at the melting point, [3.4.6.4] diagrammed in Figure 2, has an area

$$A(\text{convex hull}) = 22.069796$$

and

$$A(\text{minimal hexagon}) = 25.856406$$

We associated two tessellations with the geometry at the freezing point, shown in Figures 4 and 5. For the tessellation [3.6.3.6] diagrammed in Figure 5,

$$A(\text{convex hull}) = 15.141593$$

and

$$A(\text{minimal hexagon}) = 18.473709$$

Corresponding to the case $n = 5$ (net 5), with the tessellation shown in Figure 3,

$$A(\text{convex hull}) = 18.60569$$

and

$$A(\text{minimal hexagon}) = 23.367100$$

Because the ordered arrays bracketing the transition region have internal gaps, these configurations are not optimal Groemer packings: on the dense fluid side, the difference between the values of A(convex hull) and A(minimal hexagon) is 22.0%; on the solid side, the difference is 17.2%.

In the transition region, the disparity between the area of the optimal Groemer disk packing and the minimal hexagonal area of the array, Figure 3, is 25.6%, larger than either of the bracketing configurations. We expect that randomly distributed, and arbitrarily configured clusters in the transition region will be characterized by even larger area differences, relative to the closest space spanning tessellation. In classical free volume theories of the liquid state, these area differences translate into entropy differences, thus providing the driving force for the transition(s).

IV. Characteristics of the Transition Region

In the preceding sections two different signatures of possible disk configurations were explored, the density (packing fraction) and the free volume. One finds, first, as one changes from net 6 to net 5 to net 4 or net 3, that the packing fraction passes through a shallow minimum. And, second, area deviations from the optimal Groemer packing are larger for a configuration descriptive of the hexatic region than for either the liquid just before the transition to the hexatic or for the solid just before transition to the hexatic.

We stress that these two measures were quantified for a particular set of 2D space spanning tessellations that, by virtue of percolated disk-disk contacts, are tightly packed and spatially ordered. Although voids occur in these configurations [Figures 1−5], they are the consequence of nearest-neighbor alignments induced by hard-core repulsions only; attractive interactions between disks that can stabilize more open configurations (and influence the disk transition) are totally suppressed. Morphologically, passage from a region of higher- to lower-packing fraction relaxes the geometrical constraints induced by tightly packed disk configurations, resulting in a variety of possible spatial structures between or among which transitions can occur. The physical idea on which this paper is based is that certain 2D space spanning tessellations provide a reference frame in terms of which these intermediate structures can be compared.

To translate this physical idea into an operational strategy, the conceptual motif of renormalization theory provides a natural language. The sequential removal of disks corresponds to a "thinning out" of degrees of freedom of a system, and the subsequent rescaling of the fundamental unit area corresponds to a length renormalization. Taken together, the sequence of 2D space spanning tessellations displayed in Figures 1−5 is the consequence of implementing this procedure.

The overall physical picture of the disk transition that then emerges from the geometrical considerations outlined in this paper is the following. Starting from the dense fluid, the transition to the hexatic phase occurs at a packing fraction of ∼0.680, with the possibility of forming a 2D space spanning tessellation, the regular polygonal structure described by the planar net [3.6.3.6] (the Kagome net). However, the same packing fraction also characterizes a tessellation related to but distinct from the Kagome net, viz., [3.6.3.6,$(3^2.6^2)^2$]. Thus, at the packing fraction ∼0.680, the existence of two space spanning tessellations with distinct symmetries is a geometric analogue of the bifurcation of solutions to an underlying nonlinear equation.[27] For packing fractions exceeding ∼0.680, one enters a domain where the possible 2D space spanning extended arrays that dominate the structural landscape do not have regular polygons only. Rather, three, four and five sided polygons with variable angle and variable bond length are found.

At a packing fraction of ∼0.729, the tessellation that spans the system has an ordered array of (again) regular polygons, specified by the lattice [3.4.6.4]. Viewed from the high-density side, we associate this packing fraction with the onset of the solid-to-hexatic transition.

The previously noted, nonmonotonic behavior [eq 14] of the packing fraction as a function of n, the number of disks in the smallest confining hexagon, is reminiscent of a van der Waals loop in the behavior of the compressibility factor as a function of density. In the classical view of a phase transition, a van der Waals loop, coupled with an attendant convention [e.g., the Maxwell construction] links two physically distinct states of different density. The van der Waals loop region is conventionally considered to be metastable. In contrast, the intermediate region we identify with the hexatic phase links the liquid state with packing fraction ∼0.680 with the solid state with packing fraction ∼0.729 via equilibrium states.

V. Discussion

In this section we comment on the possible relationship between previous studies of transitions in two-dimensional systems and this study. The study of phase transitions using the "lattice gas" model leads to an unambiguous characterization of the transition on, for example, square-planar[3] and hexagonal[4] lattices. In fact, taken in tandem with earlier results of Domb,[28] Shrock and Wu[29] have calculated exactly the factor that links the spanning tree entropy for square, hexagonal, triangular and Kagome lattices with the free energy of the Ising model at the critical point. The transition is second order with a divergent correlation length. The emergence of a second-order transition

in these lattice systems is predicated on the assumption that the geometry of the species is congruent with the underlying lattice structure. A natural question that arises is what happens in the event that the geometry of the unit is not congruent with the underlying lattice structure. Or, as put by Frenkel et al.,[5] *"How does a liquid freeze if the geometry of its particles conflicts with the symmetry of the crystal it should naturally form."* In a Monte Carlo study of hard pentagons, these authors document that the equation of state shows two discontinuities, one at a low density and one at a higher density. Thus, the phase behavior they uncover is analogous to the behavior found by Mak[6] in his Monte Carlo simulations of 2D hard disks. Taken together, the results of the two studies are consistent with the characterization of the hexatic phase identified here, where the regular polygonal configurations characterizing freezing and melting bound a regime organized (in part) as clusters of hard disks configured in nonregular pentagonal arrays.

The ideas presented here may also be linked with those underlying the KTHNY theory of 2D melting. In KTHNY theory, the transition region is characterized by a long-range hexagonal order, but, locally, there exist configurations of 5-particle and 7-particle clusters that, taken together, average out to a hexagonal-like phase, the hexatic phase. A parameter, useful in characterizing the hexatic phase, is the bond orientation function ψ that, for a reference triangular lattice, is defined as

$$\psi_6 = \left| \frac{1}{N} \sum_{i=1}^{N} \frac{1}{N_i} \sum_{j} e^{li\vartheta_{ij}} \right| \tag{16}$$

Here, N is the number of disks, ϑ_{ij} is the angle between the bond connecting particles i and j and an arbitrary, but fixed, reference axis, and the sum on j is over the N_i nearest neighbors of i. As noted by Binder and Kob,[30] the global ψ in the KTHNY scenario should be strictly zero in the region between the liquid and solid densities.

Considering first the tessellation [3.4.6.4] corresponding to the packing fraction 0.729, each of the six disks (vertices) in the unit cell (diagrammed in O'Keeffe and Hyde[22]) has the designation [3.4.6.4]. Choosing one "*leg*" of one square as the reference axis, and tracing counterclockwise, the four angles circling any given vertex are 0, $\pi/3$, $5\pi/6$ and $3\pi/2$. The value of ψ calculated for this set of angles for the designated vertex is exactly zero (as it is for the other disks in the unit cell). Similar calculations based on the unit cell characterizing other tessellations in the range of packing fractions considered in this study are listed in Table 2. Calculation of ψ for various configurations displayed in the panels of Figure 6 gives values bounded from above by ~0.40. These results lend support to the conjecture that the space-spanning disk tessellation [3.4.6.4] signals the onset of the hexatic phase.

There is further evidence for the (perhaps) central role of the tessellation [3.4.6.4] in the melting transition. If one computes the second nearest-neighbor distance (X) between disks that are centered on the vertices of [3.4.6.4], one calculates $X/\sigma = 1.932$. This value is remarkably close to the value of X/σ characterizing the location of the shoulder in the representation of the radial distribution function as a function of the reduced density which Truskett et al.[12] observed to develop first in the vicinity of the freezing transition, and then become more and more prominent as one approaches the melting transition.

Finally, we return to the question of what connection, if any, exists between the hexatic phase and the (nonregular) polygonal configurations defining the representative array [5.4^3, 5.4.3.4, 5.4^3, $(5.4.3.4)^2$]. As may be seen in Figure 5, "erasing" just a few lattice bonds in the crystallographic unit cell defining the array [5.4^3, 5.4.3.4, $5.4^3(5.4.3.4)^2$] results in 8 constellations of 5-disk clusters, 3 constellations of 6-disk clusters, and 8 constellations of 7-disk clusters, an overall average of "*6.*" Hence, from a structural point of view, there is no apparent contradiction between the KTHNY theory and the geometric interpretation presented here.

TABLE 2: Packing Fraction and ψ (Unit Cell) for Selected Tessellations

tessellation	packing fraction	ψ
hexagonal lattice [6^3]	$\pi/27^{1/2} = 0.6046$	1
Kagome tiling [$(3^2.6^2)^4$, $(6^3)^3$, $(3.6.3.6)^5$]	$11\pi/(30\cdot 3^{1/2} = 0.6651$	1
Kagome net [3.6.3.6]	$3^{1/2}\pi/8 = 0.6802$	1
Kagome lattice [3.6.3.6, $(3^2.6^2)^2$]	$= 0.6802$	1
tungsten bronze (tetrahedral) 5.4^3,(5.4.3.4),(5.4^3),$(5.4.3.4)^2$]	$= 0.6775$	0.238
[$(3.5.4.5)^2$,(3.5.3.5)]	$= 0.679$	0.287
MacMahon's coordinates [$(5^3)^2$, 5^4, 5^3, 5^4]	$= 0.709$	0.393
[3.4.6.4]	$3^{1/2}\pi/4 + 2\cdot 3^{1/2} = 0.7290$	0
[$(3.4.5.4)^2$, $(3.5.4.5)^2$]	$= 0.751$	0.376
square-planar lattice	$\pi/4^{1/2} = 0.7854$	
triangular lattice [3^6]	$\pi/2^{1/2} = 0.9069$	1

Acknowledgment. We thank Professor Robert Shrock of State University of New York at Stony Brook, Professor Erich Friedman of Stetson University and Professor Shu-Chiuan Chang of National Cheng Kung University (Taiwan) for helpful suggestions and/or clarifications. This research was supported by the NSF funded MRSEC Laboratory at The University of Chicago.

Appendix

The simulations described in the text were rendered using Autodesk's Maya package. Each particle was represented (generated) as a spherical rigid body, placed on a plane. The parameters of the simulation were selected to render observable the intermediate states of the transition we wished to study. A small force, perpendicular to the plane was applied to all spheres in the simulation, to ensure that they always remain in contact with the plane, i.e., to make sure that the transition occurs in 2D. Each sphere was a rigid body with an assigned mass of 1. The elasticity coefficient for sphere−sphere collisions was set to 0.6 and static friction and dynamic friction coefficients were set to 0.6. To simulate a transition between two lattices, we placed the spheres so that their centers were initially located over the vertices of the lattice that defines the starting configuration of the system. On each node of the target lattice, a force was applied such that the sphere centers rolled into positions directly over the vertices of the target lattice. These forces were always parallel to the plane. The steps in the simulation of the transition from the initial lattice to the target lattice were repeated until movement of the spheres ceases to occur. Typically, all spheres settled over vertices of the target lattice after 5000 frames, executed at 24 frames/second.

References and Notes

(1) Alder, B. J.; Wainwright, T. E. *Phys. Rev.* **1962**, *127*, 359.

(2) Alder, B. J.; Hoover, W. G.; Wainwright, T. E. *Phys. Rev. Lett.* **1963**, *11*, 241.

(3) (a) Burley, D. M. *Proc. R. Philos. Soc. (London)* **1960**, *75*, 262. (b) Runnels, L. K. *Phys. Rev. Lett.* **1965**, *15*, 581. (c) Gaunt, D. A.; Fisher, M. E. *J. Chem. Phys.* **1965**, *43*, 2840. (d) Bellemans, A.; Nigam, R. K. *Phys. Rev. Lett.* **1966**, *16*, 1038.

(4) (a) Baxter, R. J. *J. Phys. A: Math. Gen.* **1980**, *13*, L61. (b) Baxter, R. J. *J. Stat. Phys.* **1981**, *26*, 427. (c) Baxter, R. J. *Exactly Solved Models in Statistical Mechanics*; Academic Press: London, 1982.

(5) Schilling, T.; Pronk, S.; Mulder, B.; Frenkel, D. *Phys. Rev.* **2005**, *E 71*, 036138.

(6) Mak, C. H. *Phys. Rev.* **2006**, *E73*, 065104(R)

(7) Kosterlitz, J. M.; Thouless, D. J. *J. Phys. (Paris)* **1972**, *C5*, l124.

(8) Halperin, B. I.; Nelson, D. R. *Phys. Rev. Lett.* **1978**, *41*, 121.

(9) Nelson, D. R.; Halperin, B. I. *Phys. Rev.* **1979**, *B 19*, 2457.

(10) Young, A. P. *Phys. Rev.* **1979**, *B 19*, 1855.

(11) For a review, see: : Nelson D. R. In *Phase Transition and Critical Phenomena*; Domb, C., Lebowitz, J. L., Eds.; Academic: London, 1983; Vol. 7.

(12) Truskett, T. M.; Torquato, S.; Sastry, S.; Debenedetti, P. G.; Stillinger, F. H. *Phys. Rev.* **1998**, *E 58*, 3083.

(13) Huerta, A.; Naumis, G. G. *Phys. Rev. Lett.* **2003**, *90*, 145701.

(14) Huerta, A.; Naumis, G. G.; Wasan, D. T.; Henderson, D.; Trokhymchuk, A. *J. Chem. Phys.* **2004**, *120*, 1506.

(15) Moucka, F.; Nezbeda, I. *Phys. Rev. Lett.* **2005**, *94*, 040601.

(16) Huerta, A.; Henderson, D.; Trokhymchuk, A. *Phys. Rev. E* **2006**, *74*, 061106.

(17) Fejes Toth, L. *Regular Figures*; The MacMillan Company: New York, 1964.

(18) Groemer, H. *Math.Z.* **1960**, *73*, 285.

(19) Wegner, G. *Studia Sci. Math. Hungar.* **1986**, *21*, 1.

(20) Croft, H. T.; Falconer, K. J.; Guy, R. K. *Unsolved Problems in Geometry*; Springer-Verlag: New York, 1991; p 117.

(21) See: Friedman, E. "Circles in Triangles". http://www.stetson.edu/~efriedma/cirintri/.

(22) O'Keeffe, M.; Hyde, G. G. *Philos. Trans. R. Soc. (London), Ser. A* **1980**, *295*, 553.

(23) See: Friedman, E. "Circles in Hexagons". http://www.stetson.edu/~efriedma/cirinhex/.

(24) Penrose, R. *Bull. Inst. Math. Appl.* **1974**, *10*, 266.

(25) Henley, C. L. *Phys. Rev. B* **1986**, *34*, 797.

(26) Hyde, B. G.; Bursill, L. A.; O'Keeffe, M.; Anderson, S. *Nature* **1972**, *237*, 35.

(27) See the following, and references cited therein: (a) Weeks, J. D.; Rice, S. A.; Kozak, J. J. *J. Chem. Phys.* **1970**, *52*, 2416. (b) Kozak, J. J. *Adv. Chem. Phys.* **1979)** , *40*, 229. (c) Bagchi, B.; Cerjan, C.; Rice, S. A. *Phys. Rev.* **1983**, *B 28*, 6411. (d) Haymet, A. D. J. *Annu. Rev. Phys. Chem.* **1987**, *38*, 89. (e) Baus, M. and ; Tejero, C. F. *Equilibrium Statistical Mechanics: Phases of Matter and Phase Transitions*; Springer: New York, 2008.

(28) Domb, C. *Adv. Phys.* **1960**, *9*, 149–361.

(29) Shrock, R.; Wu, F. Y. *J. Phys. A: Math. Gen.* **2000**, *33*, 3881.

(30) Binder, K.; Kob, W. *Glassy Materials and Disordered Solids*; World Scientific Publishing Co., pte. Ltd.: Singapore, xxxx.

JP806287E